Brain glucose and acetoacetate metabolism: a comparison of young and older adults

Scott Nugent [a,b,*], Sebastien Tremblay [a,e], Kewei W. Chen [f], Napatkamon Ayutyanont [f],
Auttawut Roontiva [f], Christian-Alexandre Castellano [a,b], Melanie Fortier [a], Maggie Roy [a,b],
Alexandre Courchesne-Loyer [a,b], Christian Bocti [a,d], Martin Lepage [c,e], Eric Turcotte [c,e],
Tamas Fulop [a,b,d], Eric M. Reiman [f], Stephen C. Cunnane [a,b,d]

[a] Research Center on Aging, Université de Sherbrooke, Sherbrooke, Quebec, Canada
[b] Department of Physiology and Biophysics, Université de Sherbrooke, Sherbrooke, Quebec, Canada
[c] Department of Nuclear Medicine and Radiobiology, Université de Sherbrooke, Sherbrooke, Quebec, Canada
[d] Department of Medicine, Université de Sherbrooke, Sherbrooke, Quebec, Canada
[e] Sherbrooke Molecular Imaging Center, Université de Sherbrooke, Sherbrooke, Quebec, Canada
[f] Banner Alzheimer's Institute, Phoenix, AZ, USA

ARTICLE INFO

ABSTRACT

The extent to which the age-related decline in regional brain glucose uptake also applies to other important brain fuels is presently unknown. Ketones are the brain's major alternative fuel to glucose, so we developed a dual tracer positron emission tomography protocol to quantify and compare regional cerebral metabolic rates for glucose and the ketone, acetoacetate. Twenty healthy young adults (mean age, 26 years) and 24 healthy older adults (mean age, 74 years) were studied. In comparison with younger adults, older adults had $8 \pm 6\%$ (mean $\pm$ SD) lower cerebral metabolic rates for glucose in gray matter as a whole ($p = 0.035$), specifically in several frontal, temporal, and subcortical regions, as well as in the cingulate and insula ($p \leq 0.01$, false discovery rate correction). The effect of age on cerebral metabolic rates for acetoacetate in gray matter did not reach significance ($p = 0.11$). Rate constants (min^{-1}) of glucose (Kg) and acetoacetate (Ka) were significantly lower ($-11 \pm 6\%$; [$p = 0.005$], and $-19 \pm 5\%$; [$p = 0.006$], respectively) in older adults compared with younger adults. There were differential effects of age on Kg and Ka as seen by significant interaction effects in the caudate ($p = 0.030$) and post-central gyrus ($p = 0.023$). The acetoacetate index, which expresses the scaled residuals of the voxel-wise linear regression of glucose on ketone uptake, identifies regions taking up higher or lower amounts of acetoacetate relative to glucose. The acetoacetate index was higher in the caudate of young adults when compared with older adults ($p \leq 0.05$ false discovery rate correction). This study provides new information about glucose and ketone metabolism in the human brain and a comparison of the extent to which their regional use changes during normal aging.

© 2014 Elsevier Inc. All rights reserved.

1. Introduction

In cognitively normal older adults, glucose uptake measured by positron emission tomography (PET) using ^{18}F-fluorodeoxyglucose (FDG) has been reported to be lower in several brain regions relative to young adults, particularly in the precuneus, posterior cingulate, and parietal, temporal and frontal cortex (De Santi et al., 1995; Marano et al., 2012; Willis et al., 2002; Yanase et al., 2005). However, after correction for partial volume effects (PVE) mainly because of regional brain atrophy with age, either FDG uptake is no longer significantly different (Curiati et al., 2011; Ibanez et al., 2004; Yanase et al., 2005), or the only region in which FDG uptake remains significantly lower is in the frontal cortex (Kalpouzos et al., 2009). Lower regional glucose uptake is more pronounced in Alzheimer's disease, and may be of some use in the differential diagnosis of specific forms of aging-associated cognitive impairment (Chetelat et al., 2013; Kantarci et al., 2010; Li et al., 2008; Mosconi et al., 2009; Scheef et al., 2012). Lower regional brain glucose uptake is also present in young adults with a maternal family history of Alzheimer's disease (Mosconi et al., 2007) or with a genetic predisposition to Alzheimer's disease by

* Corresponding author at: Research Center on Aging, 1036 Belvedere St. South, Sherbrooke, QC, Canada J1H 4C4. Tel.: +1 819 780 2220; fax: +1 819 829 4171.
E-mail address: stephen.cunnane@usherbrooke.ca (S.C. Cunnane).

virtue of carrying the apolipoprotein E ε4 allele (Reiman et al., 2004, 2005).

Glucose is the brain's predominant fuel under normal conditions but it is not the brain's only fuel (Cunnane et al., 2011; Gottstein et al., 1971; Owen et al., 1967). The ketones, acetoacetate [AcAc], and β-hydroxybutyrate are the brain's main alternative fuels to glucose in adult humans and are essential brain fuels during infant development (Cremer, 1982; Nehlig, 2004; Robinson and Williamson, 1980). In adult humans, plasma ketones commonly reach 2–3 mM during 3–6 days fasting, prolonged exercise, or on a very high fat ketogenic diet (Balasse and Fery, 1989; Cahill, 2006; Mitchell et al., 1995; Owen et al., 1967). The ketogenic response to fasting is essential to preserve muscle protein, which would otherwise be depleted to produce glucose for the brain from amino acids via gluconeogenesis (Veech et al., 2001). Indeed, during starvation, ketones can provide up to 70% of the brain's fuel requirements (Cahill, 2006; Hasselbalch et al., 1995; Owen et al., 1967; Robinson and Williamson, 1980). Normal brain function can be maintained by ketone infusion during acute, controlled experimental plasma glucose depletion (Amiel et al., 1991; Page and Williamson, 1971; Veneman et al., 1994).

Ketones use a different transport system to enter the brain (monocarboxylic acid transporters) than glucose (Morris, 2005; Pierre and Pellerin, 2005), and are catabolized to acetyl CoA independently of glycolysis (Mamelak, 2012; Veech et al., 2001). Unlike glucose, ketones are taken up and metabolized by the brain in direct proportion to their arterial concentration (Blomqvist et al., 2002; Cunnane et al., 2011; Hasselbalch et al., 1996). Glucose metabolism is largely separate from ketone metabolism but some carbon from glucose can be incorporated into ketones via acetyl CoA (Laffel, 1999). However, conditions that increase plasma glucose generally also increase plasma insulin which is the main inhibitor of ketone synthesis, thereby usually insuring that acetyl CoA from glucose goes either to the Krebs' cycle or to amino acid synthesis but not to ketogenesis.

Without measuring uptake of at least one other fuel that is taken up by the brain independently of glucose, it remains unclear as to whether lower brain glucose uptake in healthy older adults or in those at risk of Alzheimer's disease can be interpreted as being a generalized marker of deteriorating brain energy metabolism or could possibly be specific to glucose. Some brain regions taking up less glucose in older adults might still be functional but cannot obtain or metabolize enough glucose because of a problem related to glucose transport or usage (Cunnane et al., 2011; Maalouf et al., 2009; Mamelak, 2012; Swerdlow, 2009). If that were the case, a fuel accessing the tricarboxylic acid cycle independently of glycolysis, that is ketones, would not necessarily display the same pattern of brain hypometabolism as glucose. Equally importantly, brain regions that apparently take up glucose normally during aging may not necessarily be able to adequately take up ketones, yet both are important for optimal brain function.

We therefore developed carbon-11 acetoacetate (^{11}C-AcAc) as a PET ketone tracer (Tremblay et al., 2007) to use in parallel with FDG in studying brain energy metabolism during aging. Our objective was to assess the extent to which the regional pattern of brain ^{11}C-AcAc uptake resembles that of FDG in healthy, cognitively normal young and older adults. We established a brain PET protocol in which ^{11}C-AcAc is the first tracer injected because of its shorter half-life of [11]C (20 minutes), followed by a wash-out period and then injection of FDG. PET images were co-registered to each participant's respective magnetic resonance (MR) images, and brain regions were segmented for quantitative PET tracer uptake analysis after PVE correction (Quarantelli et al., 2004).

The tracer uptake data was expressed in 3 ways: (1) cerebral metabolic rate (μmol/100 g/min) of glucose (CMRg), and AcAc (CMRa); (2) rate constants (min^{-1}) of glucose (Kg) and AcAc (Ka), and; (3) the acetoacetate index (AI). CMR is the traditional measure for quantifying brain fuel uptake and is the product of K multiplied by the plasma concentration of the metabolite in question. Plasma ketones vary markedly even under well-controlled conditions and so directly influence CMRa variability, thereby potentially masking differences with age (Lying-Tunell et al., 1981). Reporting the Ka considerably reduces this variability and potentially reveals differences in brain AcAc uptake not otherwise detectable. The AI is based on the approach of Vaishnavi et al. (2010) in which the scaled residuals of the voxel-wise linear regression of glucose on ketone uptake identify regions of the brain taking up higher or lower amounts of ^{11}C-AcAc relative to FDG.

2. Methods

2.1. Participants

Ethical approval for this study was obtained from the Research Ethics Committee of the Health and Social Services Center–University of Sherbrooke Geriatrics Institute, which oversees all human research at the Research Center on Aging. All participants provided written informed consent before study entry. Participants were between either 18–30 years old (young group; n = 20), or 65–85 years old (older adult group; n = 24). They all underwent a pre-screening visit, which included blood analysis based on a blood sample collected after an overnight fast, and completion of a medical history questionnaire. Exclusion criteria included a Mini-Mental State Examination (MMSE; Folstein et al., 1975) score <26/30, smoking, diabetes, or glucose intolerance (elevated fasting plasma glucose, insulin or glycated hemoglobin), evidence of overt heart, liver or renal disease, and untreated hypertension, dyslipidemia, or thyroid disease. None of the young participants were medicated. Ten of the 24 older adult participants were medicated, 7 for hypertension (irbesartan, ramipril, or telmisartan), 2 for osteoporosis (risedronate), and 2 with a gastric acid secretion inhibitor (pantoprazole).

2.2. Magnetic resonance imaging

For each participant, three-dimensional T_1-weighted MR images were acquired on a 1.5 Tesla scanner (Sonata, Siemens Medical Solutions, Erlangen, Germany). The parameters of the gradient echo sequence were: repetition time/echo time - 16.00/4.68 ms, 20° flip angle, 1 mm^3 isotropic reconstructed voxel size, $256 \times 240 \times 192$ mm^3 field of view, matrix size of $256 \times 256 \times 164$, number of averages of 1, and an acquisition time of 9.14 minutes. A set of 20 fluid attenuated inversion recovery images were also acquired in the axial direction. The parameters were: repetition time/echo time - 8500/91 ms, 2400 ms inversion time, echo train length of 17, matrix size of 256×192, for a 230×172.5 mm^2 field of view, slice thickness of 6 mm, spacing between slices of 1.2 mm, number of acquisitions of 1, and an acquisition time of 3.09 minutes. Fluid attenuated inversion recovery MR images of the brain were reviewed by a neurologist and no evidence of structural abnormality was found in any young or older adult participant.

2.3. PET and cerebral metabolic rates

[11]C-AcAc was synthesized as described previously (Tremblay et al., 2007). Brain PET scans were performed on a Philips Gemini TF PET/CT scanner (Philips Medical System, Eindhoven, The Netherlands) using a dynamic list mode acquisition, with time-of-flight enabled, an isotropic voxel size of 2 mm^3, field-of-view of 25 cm, and an axial field of 18 cm. For ^{11}C-AcAc, the time frames

Table 1
Characteristics of the study participants

Characteristics	Young adults (n = 20)		Older adults (n = 24)		
	Mean	SD	Mean	SD	p
Age (y)	26	4	74	5	*
Sex (M/F)	11/9	-	8/16	-	
Blood pressure (mm/Hg)					
Systolic	110	12	134	17	*
Diastolic	70	10	81	14	
Heart rate (beats/min)	63	9	67	10	
Height (cm)	174	9	164	10	*
Weight (kg)	71	14	71	16	
Body mass index (kg/m^2)	23	3	26	4	*
Mini mental state exam (/30)	29.8	0.6	29.1	1.0	
Fasting plasma measurements					
Glucose (mM)	5.0	0.4	5.2	0.5	
Acetoacetate (mM)	0.15	0.10	0.12	0.04	
β-Hydroxybutyrate (mM)	0.32	0.26	0.21	0.10	
Cholesterol (mM)	4.4	1.1	4.7	1.2	
Triglycerides (mM)	0.8	0.4	0.8	0.4	
Free fatty acids (mM)	0.8	0.2	0.9	0.2	
Insulin (IU/L)	4.4	2.2	5.2	2.3	
Hemoglobin A1$_c$ (%)	5.2	0.2	5.8	0.3	*
Albumin (g/L)	46	3	43	2	*
Aspartate aminotransferase (IU/L)	24	12	25	4	
Alanine aminotransferase (IU/L)	20	9	22	8	
Thyroid stimulating hormone (mIU/L)	2.2	0.7	2.4	0.8	
HDL cholesterol (mmol/L)	1.5	0.3	1.5	0.3	
LDL cholesterol (mmol/L)	2.3	0.8	2.9	0.9	
Creatinine (μmol/L)	73	12	71	18	

Values are mean and SD, p-values were calculated using unpaired t-test and a χ^2 test was used to evaluate sex differences between age groups, uncorrected for multiple comparisons, * p ≤ 0.05.
Key: HDL, high-density lipoprotein; LDL, low-density lipoprotein; SD, standard deviation.

were 12 × 10 seconds, 8 × 30 seconds, and 1 × 4 minutes, for a total scan length of 10 minutes, which was followed by a 50- minute wash-out period. For FDG, time frames were allocated according to 12 × 10 seconds, 8 × 30 seconds, 6 × 4 minutes, and 3 × 10 minutes, for a total scan length of 60 minutes. After breakfast, each participant fasted for 6–7 hours before scanning which was performed at around 2 PM. Each participant's head was positioned in the headrest and gently restrained with straps in a dark quiet environment. An indwelling venous catheter was introduced into a forearm vein, which was placed in a hand warmer at 44 °C (Phelps et al., 1979). A second catheter was placed in the contralateral forearm vein for the injection of 5 mCi of tracer, which was infused over 20 seconds using an infusion pump. Blood samples were obtained at 3, 6, and 8 minutes after ^{11}C-AcAc infusion and at 3, 8, 16, 24, 35 and 55 minutes after FDG infusion. Radioactivity in plasma samples was counted in a gamma counter (Cobra, Packard, United States) cross-calibrated with the PET scanner.

PET images underwent a series of preprocessing steps to produce quantitative images of brain glucose and AcAc uptake. First, PET images were automatically co-registered to each participant's respective MR image using a cross-modality 3D image fusion tool implemented in PMOD 3.3 (PMOD Technologies Ltd, Zurich, Switzerland). Co-registered PET images were then corrected for PVE using the modified Müller-Gartner method (Quarantelli et al., 2004), which is fully implemented in the PVElab software (http://nru.dk/downloads/software).

Using the PMOD 3.3 pixel-wise kinetic modeling tool (PXMOD), parametric images of CMRg and CMRa were produced for each participant. Quantification of CMR requires an arterial input function, which was determined by tracing regions of interest (ROIs) on the internal carotid arteries with the aid of co-registered MR images as previously validated in humans (Zhou et al., 2011). The calculated activity within the ROI was corrected using the radioactivity of the plasma samples obtained during PET image acquisition. The lumped constant used for the CMRg calculation was set to 0.80 (Graham et al., 2002). CMRg and CMRa were expressed as μmol/100 g/min using the graphical Patlak model (Patlak et al., 1983). CMRa was corrected for the loss of 5.9% of the initial dose of ^{11}C-AcAc that is catabolized to [11]CO$_2$ during the ^{11}C-AcAc PET scan (Blomqvist et al., 1995).
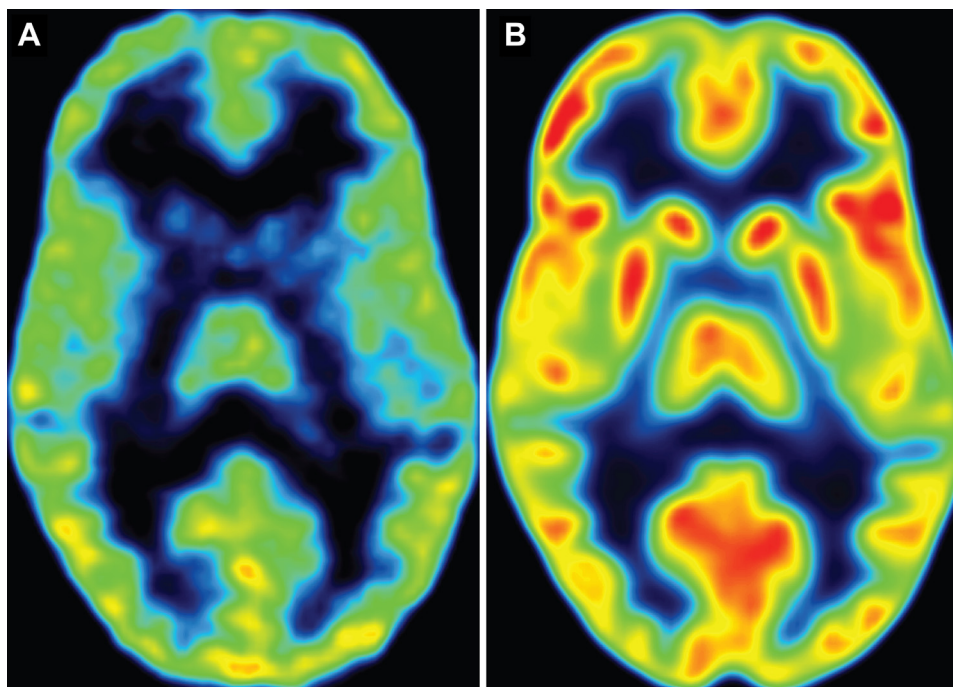

Fig. 1. Axial slices showing patterns of ^{11}C-acetoacetate (A) and ^{18}F-fluorodeoxyglucose (B) uptake in a young adult.

Using SPM8, each participant's parametric CMRg and CMRa PET images were linearly and nonlinearly deformed into the Montreal Neurological Institute (MNI) standard coordinate space using his or her MR images to estimate the spatial normalization parameters. Separate analyses were then performed for CMRg and CMRa using both ROIs and voxel-based SPM8 (http://www.fil.ion.ucl.ac.uk/spm/) analysis. For the ROI-based analysis, the data were extracted directly from the un-smoothed images for each ROI, which were predefined according to the Anatomical Automatic Labeling (AAL) template. For the voxel-based analysis, the images were smoothed by a Gaussian kernel with a full width at half maximum of 8 mm.

CMR is the product of the rate constant (K) for the tracer uptake multiplied by the plasma concentration of glucose or AcAc (Blomqvist et al., 1995, 2002). Since the plasma concentration of AcAc was relatively variable (Table 1), we report the CMR and K for both tracers. The AI was calculated as the residuals of the voxel-wise linear regression of glucose on ketone uptake ($Glucose = k \times AcAc + b$) based on the work by Vaishnavi et al. (2010). Conventionally, the AI could be calculated as the voxel-wise ratio of AcAc/glucose uptake. Because of the established statistical equivalent relationship between the ratio of AcAc/glucose and the linear regression residuals and ratio artifact for voxels with close to zero counts, we followed the approach of Vaishnavi et al. (2010) for AI computation.

2.4. Plasma metabolites

Plasma parameters were measured using an automated clinical chemistry analyzer (Dimension Xpand Plus; Siemens Healthcare Diagnostics, Deerfield, IL, USA). Plasma insulin was analyzed by commercial enzyme-linked immunosorbent assay (Alpco, Salem, NH, USA) with a Victor X4 multilabel plate reader (Perkin Elmer, Woodbridge, Ontario, Canada).

2.5. Data presentation and statistical analysis

Data are presented as mean ± SD. Levene's test was used to assess homogeneity of variance ($p \leq 0.05$) and t tests with unequal variance were used if Levene's test was significant. Brain regions refer to gray matter only, with white matter being identified separately. Two-factor analysis of variance was used to determine interaction effects between age and brain tracer uptake. Independent Student t tests were used to separately compare CMR and K between the young and older groups. These comparisons underwent a $p \leq 0.01$ false discovery rate (FDR) correction (Benjamini et al., 2001), as reported elsewhere in studies of brain glucose uptake in older adults (Esposito et al., 2008; Kalpouzos et al., 2009). Pearson correlations were performed to assess associations between CMRa or Ka and plasma AcAc, between CMRg and CMRa, and between Ka and Kg. All statistical analyses were carried out using SPSS 17.0 software (SPSS Inc, Chicago, IL, USA) except for the voxel-wise SPM8-based analysis. For the voxel-wise analysis and unless otherwise indicated, the resulting statistics at each voxel were corrected for multiple comparisons with a $p \leq 0.01$ FDR correction and displayed as SPMs in standard anatomic space, with a minimum cluster size of 50 voxels.

3. Results

The older adults were 48 years older than the young group ($p \leq 0.001$; Table 1). All anthropometric and plasma measures for both groups were within the normal range for age. However, systolic blood pressure, body mass index, and hemoglobin A1$_c$ were significantly higher whereas height and plasma albumin was significantly lower in the older adults (all $p \leq 0.05$). All participants had MMSE scores ≥29/30 and there was no difference in global cognitive status between the 2 groups as assessed by the MMSE.

Fig. 1 provides a representative example of an axial view of brain ^{11}C-AcAc and FDG uptake. In gray matter taken as a whole and compared with the young group, older adults had significantly lower CMRg ($-8 \pm 6\%$ [mean ± SD]; $p = 0.035$) but not significantly lower CMRa ($p = 0.11$) (Fig. 2A). In gray matter as a whole, Kg and Ka were both significantly lower for older adults ($-11 \pm 6\%$; $p = 0.005$, and $-19 \pm 5\%$; $p = 0.006$, respectively; Fig. 2B). On a regional basis, CMRg in the older group was 9%–15% lower specifically in the superior frontal cortex, rectus gyrus, temporal cortex, anterior cingulate, insula, putamen, and thalamus ($p \leq 0.01$ with FDR correction; Table 2). There was no significant difference in regional CMRg between men and women in our older adults, but in the young group, women had a 27% higher CMRg specifically in the posterior cingulate ($p \leq 0.001$; data not shown). Despite 20%–38% lower mean values in older adults, CMRa did not differ significantly with age in any brain region (Table 3).
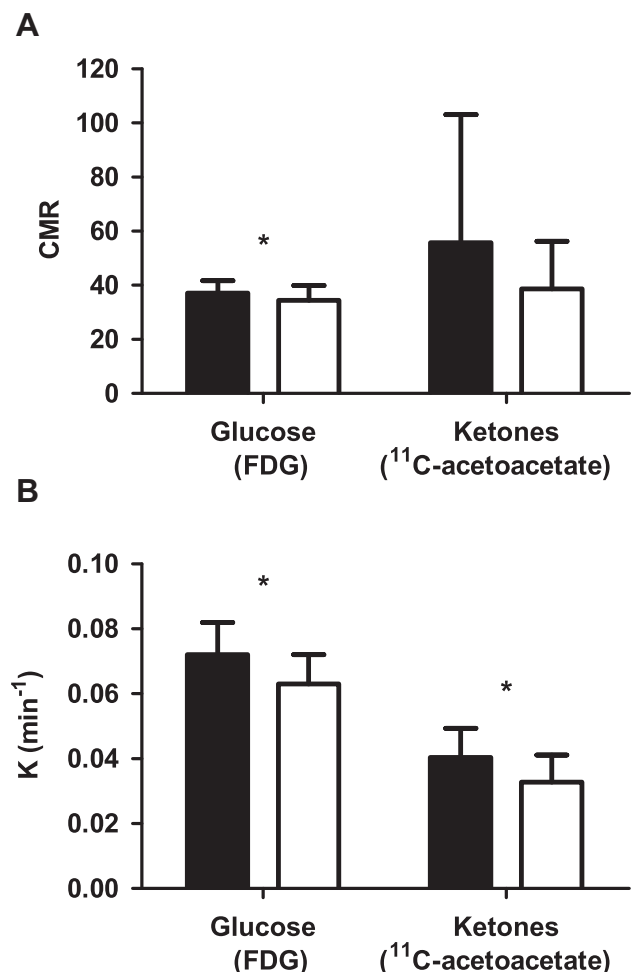

Fig. 2. Mean cerebral metabolic rate of glucose (CMRg; μmol/100 g/min) and acetoacetate (CMRa; μmol/100 g/min × 10^{-2}); (A) as well as rate constant (min^{-1}; B) for glucose (Kg) and acetoacetate (Ka) for gray matter in young (black bars) and older (white bars) adults. Older adults had significantly lower global CMRg (-8%; $p = 0.035$) but not CMRa ($p = 0.11$) when compared with young adults. Kg and Ka were both significantly lower for older adults (-11%; [$p = 0.005$], and -19%; [$p = 0.006$], respectively) when compared with young adults. Abbreviations: CMRa, cerebral metabolic rate of acetoacetate; CMRg, cerebral metabolic rate of glucose; Ka, rate constant for acetoacetate; Kg, rate constant for glucose.

Table 2
Cerebral metabolic rate of glucose (CMRg; μmol/100 g/min) and the rate constant for glucose (Kg; min^{-1}) by brain region in young and older adults

	CMRg				Kg			
	Young		Older adults		Young		Older adults	
	Mean	SD	Mean	SD	Mean	SD	Mean	SD
Cortical								
Frontal								
Frontal superior	41	6	35	8[a]	0.080	0.013	0.066	0.011[a]
Frontal medial	42	6	36	8	0.081	0.013	0.068	0.011[a]
Frontal inferior	40	5	36	7	0.079	0.011	0.066	0.009[a]
Precentral gyrus	44	6	42	9	0.085	0.013	0.079	0.012
Rectus gyrus	34	5	29	5[a]	0.066	0.010	0.053	0.009[a]
Supplementary motor	41	6	39	8	0.079	0.013	0.074	0.013
Temporal								
Superior/middle/inferior	32	4	29	4[a]	0.062	0.008	0.052	0.007[a]
Para/hippocampus	22	3	21	3	0.041	0.005	0.037	0.006
Fusiform	27	3	26	3	0.053	0.006	0.047	0.006
Parietal								
Superior/inferior	42	7	41	8	0.080	0.016	0.074	0.012
Supramarginal gyrus	38	5	35	6	0.073	0.010	0.064	0.009[a]
Postcentral gyrus	41	6	43	10	0.079	0.012	0.082	0.014
Precuneus	39	5	37	6	0.074	0.012	0.067	0.011
Angular gyrus	42	7	40	7	0.082	0.013	0.072	0.013
Occipital	38	5	37	6	0.073	0.008	0.068	0.011
Calcarine	38	5	37	5	0.074	0.009	0.067	0.011
Cuneus	41	6	42	8	0.078	0.011	0.077	0.014
Lingual	33	4	32	5	0.064	0.007	0.059	0.008
Cingulate								
Anterior	30	5	26	4[a]	0.058	0.010	0.045	0.008[a]
Middle	36	4	34	5	0.070	0.010	0.062	0.010[a]
Posterior	43	7	41	9	0.087	0.015	0.075	0.016
Rolandic operculum	34	7	31	6	0.063	0.012	0.057	0.009
Insula	31	4	28	3[a]	0.060	0.008	0.051	0.007[a]
Subcortical								
Caudate	36	7	31	6	0.072	0.011	0.058	0.011[a]
Putamen	41	6	36	6[a]	0.081	0.013	0.068	0.009[a]
Thalamus	38	6	32	5[a]	0.074	0.011	0.059	0.011[a]
Cerebellum	24	4	23	3	0.046	0.007	0.041	0.006
White matter	15	2	14	2	0.026	0.007	0.023	0.006

Mean and SD, n = 20 (young) and n = 24 (older adults).
Key: CMRg, cerebral metabolic rate of glucose; FDR, false discovery rate; Kg, rate constant for glucose; SD, standard deviation.
[a] Statistically significant difference between young and older adults after $p \leq 0.01$ FDR correction for multiple comparisons.

There was a significant interaction between Kg and Ka with age in 2 brain regions—the caudate ($p = 0.030$) and post-central gyrus ($p = 0.023$), with interactions approaching significance in the gyrus rectus ($p = 0.086$), putamen ($p = 0.094$), and thalamus ($p = 0.084$). In most brain regions, significantly lower Kg matched well with lower CMRg in older adults (Table 2). Ka was 9%–26% lower in older adults in several areas of the frontal, temporal, parietal cortex, and cingulate, as well as in the rolandic operculum, insula, and white matter ($p \leq 0.01$ FDR correction), but was not different between the 2 groups in the occipital cortex, subcortical regions (caudate, putamen, thalamus), or cerebellum (Table 3).

Plasma AcAc concentration was significantly positively correlated with CMRa for the whole brain in the young ($r = +0.96$; $p \leq 0.0001$) and older adults ($r = +0.84$; $p \leq 0.0001$), with no statistically significant difference between the slopes of the 2 regression lines ($p = 0.75$; Fig. 3A). Ka was not significantly correlated with plasma AcAc (Fig. 3B). CMRa and CMRg were significantly positively correlated across gray matter ROIs in both the young and older adult groups ($r = +0.64$ and $r = +0.73$, respectively; both $p \leq 0.0001$), and the slopes of their regression lines were not significantly different ($p = 0.09$; Fig. 4A). The equation - $CMRg = 38.30 \times CMRa + 22.54$ ($p \leq 0.001$; $r = +0.62$) describes the linear regression of the pooled CMRg and CMRa data. Kg and Ka were also significantly positively correlated across brain regions, as expressed by the following regression lines; young ($y = 1.09x + 0.03$; $r = +0.64$) and older adults ($y = 1.5x + 0.01$; $r = +0.73$; Fig. 4B).

In the young group, 9 clusters of significantly higher AI were found that encompassed mainly the bilateral caudate, putamen, precuneus, calcarine, and frontal regions ($p \leq 0.01$ FDR correction; Fig. 5A; Supplementary Table 1). Older adults had significantly higher AI localized in just 2 clusters; bilaterally in the putamen and the right caudate ($p \leq 0.01$ FDR correction; Fig. 5B; Supplementary Table 2). Subtraction of the AI map of the older adults (Fig. 5B) from that of the younger adults (Fig. 5A) revealed that our younger adults had significantly higher AI when compared with the older adults only in the caudate ($p \leq 0.05$ FDR correction; Fig. 5C; Supplementary Table 3). No regions had statistically higher (negative) AI in older adults compared with younger adults.

There was no statistically significant relationship between CMRg, CMRa, Kg or Ka, and other parameters that differed between the 2 groups, that is body mass index, systolic blood pressure, hemoglobin A1$_c$, or albumin (data not shown).

4. Discussion

This is the first report of brain uptake of ^{11}C-AcAc in humans and the first comparison of brain glucose and ketone uptake using PET in healthy older and young adults. This comparison of the uptake of the brain's two main fuels is central to the question of whether lower regional brain glucose uptake in healthy older adults is also observed with ketones, which are the brain's main alternative fuel to glucose. Our results show that there were both

Table 3
Cerebral metabolic rate of acetoacetate (CMRa; μmol/100 g/min × 10^{-2}) and the rate constant for acetoacetate (Ka; min^{-1}) by brain region in young and older adults

	CMRa				Ka			
	Young		Older adults		Young		Older adults	
	Mean	SD	Mean	SD	Mean	SD	Mean	SD
Cortical								
Frontal								
Frontal superior	56	51	36	17	0.041	0.010	0.030	0.009[a]
Frontal medial	58	51	38	18	0.042	0.010	0.032	0.009[a]
Frontal inferior	57	49	38	18	0.041	0.009	0.032	0.009[a]
Precentral gyrus	62	53	42	19	0.045	0.010	0.035	0.008[a]
Rectus gyrus	45	40	31	17	0.032	0.008	0.028	0.011
Supplementary motor	64	56	43	21	0.046	0.011	0.036	0.011[a]
Temporal								
Superior/middle/inferior	54	44	37	17	0.039	0.008	0.031	0.008[a]
Para/hippocampus	38	29	30	15	0.028	0.007	0.026	0.007
Fusiform	49	42	36	16	0.036	0.009	0.031	0.008
Parietal								
Superior/inferior	65	56	43	19	0.047	0.010	0.037	0.011[a]
Supramarginal gyrus	62	54	39	16	0.045	0.011	0.033	0.008[a]
Postcentral gyrus	65	56	44	23	0.046	0.010	0.038	0.012
Precuneus	66	54	45	21	0.048	0.010	0.038	0.010[a]
Angular gyrus	61	53	45	21	0.045	0.010	0.038	0.009
Occipital	57	47	42	20	0.041	0.008	0.036	0.009
Calcarine	66	56	46	22	0.048	0.010	0.039	0.011
Cuneus	70	57	54	27	0.051	0.010	0.046	0.012
Lingual	60	49	44	21	0.044	0.010	0.037	0.010
Cingulate								
Anterior	46	39	29	14	0.033	0.007	0.025	0.007[a]
Middle	58	52	39	19	0.042	0.010	0.033	0.009[a]
Posterior	64	60	44	23	0.048	0.022	0.037	0.016
Rolandic operculum	49	38	32	16	0.035	0.007	0.028	0.009[a]
Insula	45	37	30	14	0.033	0.008	0.025	0.007[a]
Subcortical								
Caudate	32	31	23	12	0.024	0.008	0.020	0.006
Putamen	47	43	36	18	0.034	0.010	0.030	0.009
Thalamus	53	46	38	19	0.038	0.011	0.032	0.009
Cerebellum	45	39	32	17	0.033	0.007	0.027	0.007
White matter	25	20	18	8	0.019	0.004	0.015	0.004[a]

Mean and SD, n = 20 (young) and n = 24 (older adults).
Key: CMRa, cerebral metabolic rate of acetoacetate; FDR, false discovery rate; Ka, rate constant for acetoacetate; SD, standard deviation.
  [a] Statistically significant difference between young and older adults after $p \leq 0.01$ FDR correction for multiple comparisons.

similarities and differences in the way the aging brain uses glucose and AcAc. For instance, the rate of uptake of both fuels (CMRg and CMRa) was highly correlated across brain regions (Fig. 4). Similarly, after correction for PVE and multiple comparisons, aging was associated with lower rate constants (Kg and Ka) for uptake of both fuels in gray matter taken as a whole. Regional analysis showed that lower Kg and Ka in the older group were limited in both cases mostly to the frontal, temporal and parietal cortex, as well as to the anterior and middle cingulate and the insula (Tables 2 and 3).

Despite these similarities in the aging-associated changes in regional AcAc and FDG uptakes, certain differences were also observed. There was a significant age by tracer interaction for K analysis in the caudate ($p < 0.030$) and post-central gyrus ($p < 0.023$), with interactions approaching significance in the putamen, thalamus, and gyrus rectus (Tables 2 and 3). Relative to FDG, ^{11}C-AcAc uptake was less influenced by age in the caudate, leading to proportionally higher AI in the caudate of young adults (Fig. 5). Interestingly, the caudate appears to be relatively spared from synaptic loss and resulting symptoms in Alzheimer's disease (Langbaum et al., 2009; Yuan et al., 2010). There were no sex differences in brain glucose or AcAc uptake in the elderly but, as previously reported (Andreason et al., 1994), young women had 27% higher CMRg in the posterior cingulate when compared with young men. Hence, not only is lower brain glucose uptake in those aged >70 years clearly a regional phenomenon, but the present data show that these regional changes

in brain energy metabolism with age have a certain degree of fuel specificity.

Our CMRg results agree with previous studies reporting glucose hypometabolism in frontal brain regions of older adults after correction for PVE (Kalpouzos et al., 2009). In addition to the commonly reported glucose hypometabolism in the frontal cortex, our older adults also had lower CMRg in the temporal cortex, anterior cingulate, insula, putamen, and thalamus. We also confirm the lack of aging-associated change in CMRg previously reported for white matter, cerebellum, and occipital cortex (Ibanez et al., 1998, 2004). It is not clear why there are regional differences in brain fuel uptake in cognitively healthy older adults, nor why they differ for glucose and AcAc. The ^{11}C-AcAc and FDG tracers are injected about 1 hour apart on the same day, so the reason for these differences is unlikely to be methodological. We have previously drawn attention to the fact that pyruvate dehydrogenase declines with age, which would affect glucose more than ketone usage by the tricarboxylic acid cycle (Cunnane et al., 2011).

Two previous PET studies of brain ketone uptake with the tracer, ^{11}C-β-hydroxybutyrate, have been reported (Blomqvist et al., 1995, 2002), but they made no comparison with glucose metabolism nor with age. Our results agree with Blomqvist et al. (1995) and with arterio-venous difference studies (Gottstein et al., 1971; Lying-Tunell et al., 1981) suggesting that ketones contribute to 2%–3% of the brain's total energy consumption when plasma ketones are 0.3–0.5 mM (Courchesne-Loyer et al., 2013).
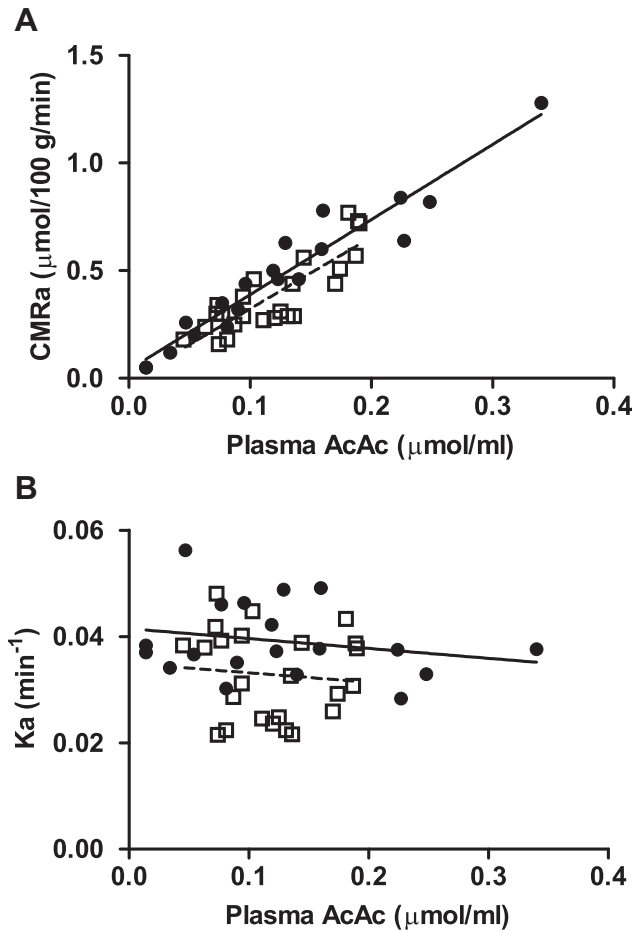
Fig. 3. Plasma acetoacetate (AcAc) plotted against mean cerebral metabolic rate of acetoacetate (CMRa; A) and the rate constant for acetoacetate (Ka; B) in gray matter. Symbols represent the mean cortical uptake for each young (●) and older (□) participant. The regression lines for the young (—; $y = 3.49x + 0.04$) and older adults (− −; $y = 3.32x − 0.01$) were not significantly different ($p = 0.75$). Abbreviations: AcAc, acetoacetate; CMRa, cerebral metabolic rate of acetoacetate; Ka, rate constant for acetoacetate.

Our brain ^{11}C-AcAc PET scans were acquired after 6 hours fasting when the sum of plasma AcAc and β-hydroxybutyrate averaged 0.45 mM. We therefore plan to repeat this experimental design before and after the participants have experienced a period of several days of mild, controlled, experimental ketonemia in which plasma ketones are raised to 1–2 mM, when brain ketone uptake should contribute up to 10%–15% of brain fuel requirements (Cunnane et al., 2011).

Brain ketone uptake varies as a function of plasma ketone concentration (Blomqvist et al., 1995; Cunnane et al., 2011; Hasselbalch et al., 1995; Owen et al., 1967), so normal inter- and intra-individual variations in plasma ketones increase the variability of CMRa. This variability in plasma ketones probably prevented us, as well as previous groups that used the arterio-venous difference approach (Gottstein et al., 1971; Lying-Tunell et al., 1981), from finding a significant difference in whole brain CMRa in older adults. To control for the variability in plasma ketones, we also expressed tracer uptake in terms of the rate constants for both FDG and ^{11}C-AcAc, Kg and Ka, respectively. Age-related differences in brain FDG uptake were minimally affected depending on whether the data were expressed as Kg or CMRg. However, the Ka revealed that lower regional brain CMRa in older adults is more a function of a lower rate constant than of plasma AcAc, because the latter did not differ significantly between the 2 groups (Table 3). Hence, somewhat higher plasma AcAc
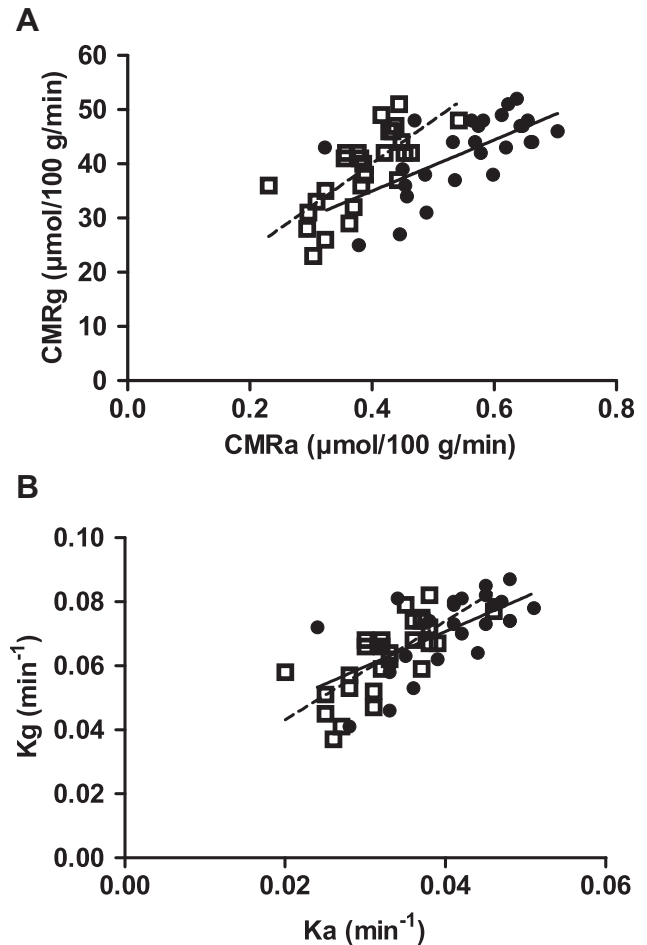

Fig. 4. Cerebral metabolic rate of acetoacetate (CMRa) plotted against the cerebral metabolic rate of glucose (CMRg). Symbols represent the mean value of each ROI (n = 28) for young (●) or older (□) adults. CMRa and CMRg were significantly positively correlated in both young and older adults ($r = +0.64$ and $r = +0.73$, respectively). The regression lines for the young (—; $y = 47.16x + 16.12$) and older adults (− −; $y = 79.54x + 14.88$) were not significantly different ($p = 0.09$). Linear regression of the pooled data was represented by $y = 38.30x + 22.54$ ($p \leq 0.001$; $r = +0.62$). Ka and Kg were significantly positively correlated in both young and older adults ($r = +0.64$ and $r = +0.73$, respectively). The regression lines for the young (—; $y = 1.09x + 0.03$) and older adults (− −; $y = 1.5x + 0.01$) were not significantly different ($p = 0.26$). Linear regression of the pooled data was represented by $y = 1.22x + 0.02$ ($p \leq 0.001$; $r = +0.72$). Abbreviations: CMRa, cerebral metabolic rate of acetoacetate; CMRg, cerebral metabolic rate of glucose; ROI, region of interest.

in older adults is needed in brain regions with a lower Ka to achieve the same net brain AcAc uptake as in younger adults.

Diets or supplements that induce mild ketosis are reportedly therapeutically beneficial in both mild cognitive impairment and Alzheimer's disease, at least on a short-term basis (Henderson, 2008; Krikorian et al., 2012; Reger et al., 2004). The present dual tracer PET protocol has potential application in assessing regional brain fuel usage in mild cognitive impairment and in Alzheimer's disease. Our present results suggest that higher ketone availability in the blood might provide a viable alternative fuel to glucose in brain regions in which glucose uptake alone was lower in older adults, that is in the rectus gyrus, caudate, putamen, and thalamus (Table 2). We have recently reported that raising plasma ketones in the rat by fasting or by a very high fat ketogenic diet increases not only brain AcAc uptake (Bentourkia et al., 2009) but also increases brain glucose uptake (Pifferi et al., 2011; Roy et al., 2012), so these results can now be tested in humans as well.
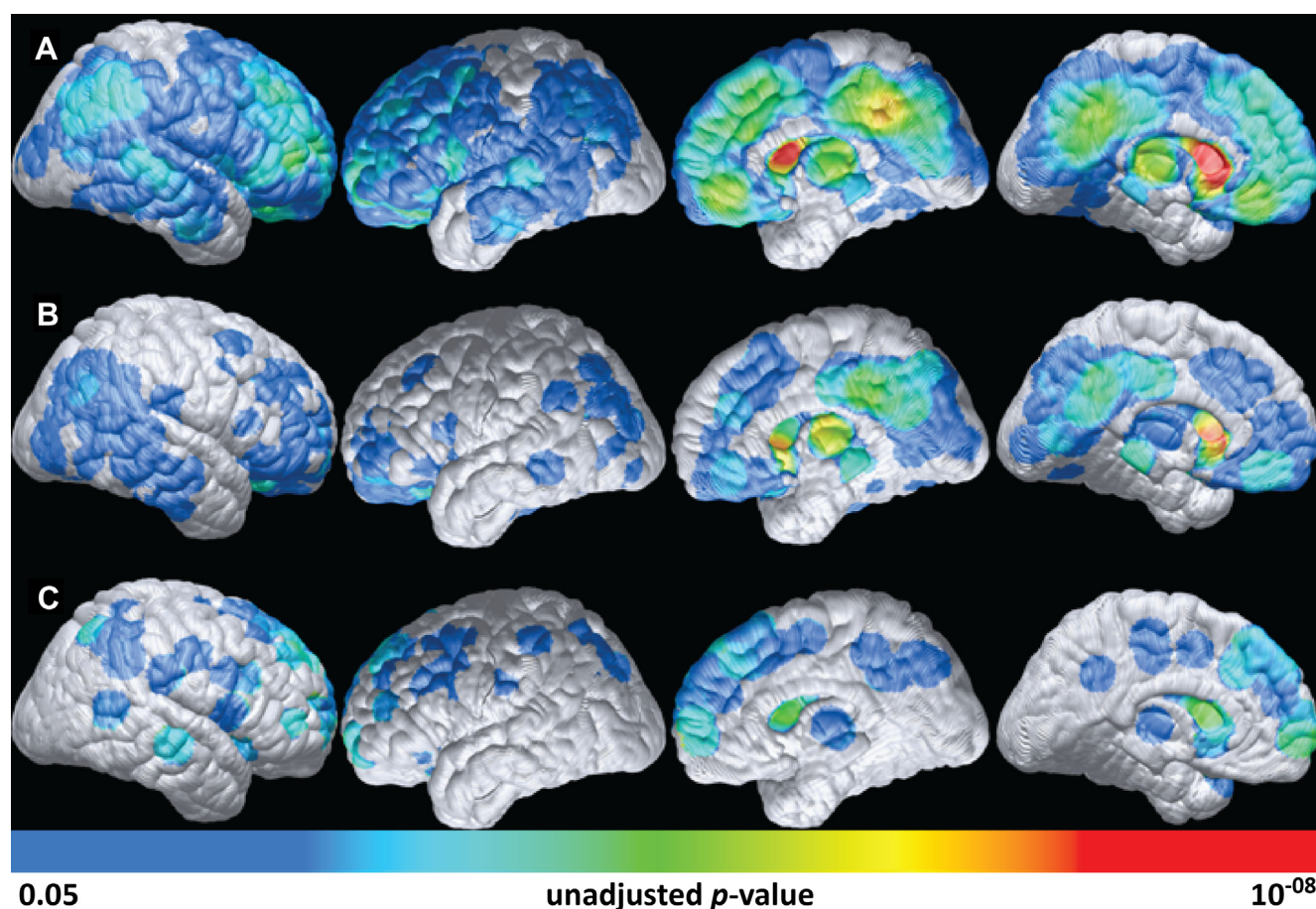
Fig. 5. Cortical surface maps of the acetoacetate index (AI) with $p \leq 0.01$ false discovery rate (FDR) correction. In young adults (A; n = 20), 9 significant clusters of high AI were present encompassing mainly the bilateral caudate, putamen, precuneus, calcarine, and frontal regions. In older adults (B; n = 24), there were 2 significant clusters of high AI—the right caudate and the right and left putamen. The difference between A and B shows that the caudate is the only cluster in which higher AI in the young group significantly exceeded higher AI in the older adult group (C; $p \leq 0.05$ FDR correction). For purposes of illustration, voxel-wise statistics surviving $p \leq 0.05$ are displayed unadjusted for multiple comparisons.

This study has several limitations. First, it did not include PET measurements of brain oxygen metabolism, so we were unable to determine the extent to which our findings could be linked to aging-related changes in aerobic glycolysis as reported elsewhere (Vaishnavi et al., 2010; Vlassenko et al., 2010). Ketone metabolism is aerobic and our AI map in young adults (Fig. 5A) is similar to the glycolytic index map reported by Vlassenko et al. (2010), suggesting that measuring brain ketone metabolism by PET with ^{11}C-AcAc may be useful in assessing whether aerobic energy metabolism in the brain changes with age. Additional studies are needed to further explore the relationships between the rates of ketone, glucose, and oxygen metabolism in young adults, as well as how these rates are affected during aging and in those predisposed to AD, and whether they are modified by ketogenic agents. Second, FDG is a relatively long-lived tracer that binds to hexokinase for which corrections are made to estimate CMRg. In contrast, ^{11}C-AcAc is not metabolically trapped but is catabolized to [11]CO$_2$, a process that consumes about 5.9% of the tracer during the 10 minutes ^{11}C-AcAc PET scan (Blomqvist et al., 1995). This difference in metabolic fate between the 2 tracers suggests that the absolute magnitudes of the aging-associated difference in brain uptake of these 2 fuels are not necessarily directly comparable except on a relative basis, which is why we also expressed the results as AI (Fig. 5). Finally, PET does not have the spatial resolution to distinguish whether some of the aging-related differences we observed were more because of changing energy metabolism in neurons or astrocytes. Astrocytes can synthesize ketones but, to our knowledge, this has only been shown in vitro and depends on exogenous medium chain (6–12 carbon) fatty acids being added in the astrocyte culture medium (Auestad et al., 1991). Although PET would not be able to evaluate ketone synthesis within astrocytes per se, under our experimental conditions, it seems unlikely that this would significantly affect our results because the ketogenic medium chain fatty acids are essentially undetectable in human plasma except in infants consuming mother's milk.

In conclusion, when expressed quantitatively and with PVE and statistical correction for multiple comparisons, the regional pattern of changing brain fuel uptake with age differs between glucose and AcAc, especially in the caudate. This study provides new information about regional glucose and ketone metabolism in the human brain and a comparison of the extent to which their use changes during normal aging.

Disclosure statement

The authors declare no actual or potential conflicts of interest.

Acknowledgements

Appendix A. Supplementary data

Supplementary data associated with this article can be found, in the online version, at http://dx.doi.org/10.1016/j.neurobiolaging.2013.11.027.

References

Amiel, S.A., Archibald, H.R., Chusney, G., Williams, A.J., Gale, E.A., 1991. Ketone infusion lowers hormonal responses to hypoglycaemia: evidence for acute cerebral utilization of a non-glucose fuel. Clin. Sci. (Lond) 81, 189–194.

Andreason, P.J., Zametkin, A.J., Guo, A.C., Baldwin, P., Cohen, R.M., 1994. Gender-related differences in regional cerebral glucose metabolism in normal volunteers. Psychiatry Res. 51, 175–183.

Auestad, N., Korsak, R.A., Morrow, J.W., Edmond, J., 1991. Fatty acid oxidation and ketogenesis by astrocytes in primary culture. J. Neurochem. 56, 1376–1386.

Balasse, E.O., Fery, F., 1989. Ketone body production and disposal: effects of fasting, diabetes, and exercise. Diabetes Metab. Rev. 5, 247–270.

Benjamini, Y., Drai, D., Elmer, G., Kafkafi, N., Golani, I., 2001. Controlling the false discovery rate in behavior genetics research. Behav. Brain Res. 125, 279–284.

Bentourkia, M., Tremblay, S., Pifferi, F., Rousseau, J., Lecomte, R., Cunnane, S., 2009. PET study of 11C-acetoacetate kinetics in rat brain during dietary treatments affecting ketosis. Am. J. Physiol. Endocrinol. Metab. 296, E796–E801. http://dx.doi.org/10.1152/ajpendo.90644.2008.

Blomqvist, G., Alvarsson, M., Grill, V., Von Heijne, G., Ingvar, M., Thorell, J.O., Stone-Elander, S., Widen, L., Ekberg, K., 2002. Effect of acute hyperketonemia on the cerebral uptake of ketone bodies in nondiabetic subjects and IDDM patients. Am. J. Physiol. Endocrinol. Metab. 283, E20–E28. http://dx.doi.org/10.1152/ajpendo.00294.2001.

Blomqvist, G., Thorell, J.O., Ingvar, M., Grill, V., Widen, L., Stone-Elander, S., 1995. Use of R-beta-[1-11C]hydroxybutyrate in PET studies of regional cerebral uptake of ketone bodies in humans. Am. J. Physiol. 269 (5 Pt 1), E948–E959.

Cahill Jr., G.F., 2006. Fuel metabolism in starvation. Annu. Rev. Nutr. 26, 1–22. http://dx.doi.org/10.1146/annurev.nutr.26.061505.111258.

Chetelat, G., Landeau, B., Salmon, E., Yakushev, I., Bahri, M.A., Mezenge, F., Perrotin, A., Bastin, C., Manrique, A., Scheurich, A., Scheckenberger, M., Desgranges, B., Eustache, F., Fellgiebel, A., 2013. Relationships between brain metabolism decrease in normal aging and changes in structural and functional connectivity. Neuroimage 76, 167–177. http://dx.doi.org/10.1016/j.neuroimage.2013.03.009.

Courchesne-Loyer, A., Fortier, M., Tremblay-Mercier, J., Chouinard-Watkins, R., Roy, M., Nugent, S., Castellano, C.A., Cunnane, S.C., 2013. Stimulation of mild, sustained ketonemia by medium-chain triacylglycerols in healthy humans: estimated potential contribution to brain energy metabolism. Nutrition 29, 635–640. http://dx.doi.org/10.1016/j.nut.2012.09.009.

Cremer, J.E., 1982. Substrate utilization and brain development. J. Cereb. Blood Flow Metab. 2, 394–407. http://dx.doi.org/10.1038/jcbfm.1982.43.

Cunnane, S., Nugent, S., Roy, M., Courchesne-Loyer, A., Croteau, E., Tremblay, S., Castellano, A., Pifferi, F., Bocti, C., Paquet, N., Begdouri, H., Bentourkia, M., Turcotte, E., Allard, M., Barberger-Gateau, P., Fulop, T., Rapoport, S.I., 2011. Brain fuel metabolism, aging, and Alzheimer's disease. Nutrition 27, 3–20. doi:S0899-9007(10)00280-7 [pii]. 10.1016/j.nut.2010.07.021.

Curiati, P.K., Tamashiro-Duran, J.H., Duran, F.L., Buchpiguel, C.A., Squarzoni, P., Romano, D.C., Vallada, H., Menezes, P.R., Scazufca, M., Busatto, G.F., Alves, T.C., 2011. Age-related metabolic profiles in cognitively healthy elders: results from a voxel-based [18F]fluorodeoxyglucose-positron-emission tomography study with partial volume effects correction. AJNR Am. J. Neuroradiol. 32, 560–565. http://dx.doi.org/10.3174/ajnr.A2321.

De Santi, S., de Leon, M.J., Convit, A., Tarshish, C., Rusinek, H., Tsui, W.H., Sinaiko, E., Wang, G.J., Bartlet, E., Volkow, N., 1995. Age-related changes in brain: II. Positron emission tomography of frontal and temporal lobe glucose metabolism in normal subjects. Psychiatr. Q. 66, 357–370.

Esposito, G., Giovacchini, G., Liow, J.S., Bhattacharjee, A.K., Greenstein, D., Schapiro, M., Hallett, M., Herscovitch, P., Eckelman, W.C., Carson, R.E., Rapoport, S.I., 2008. Imaging neuroinflammation in Alzheimer's disease with radiolabeled arachidonic acid and PET. J. Nucl. Med. 49, 1414–1421. http://dx.doi.org/10.2967/jnumed.107.049619.

Folstein, M.F., Folstein, S.E., McHugh, P.R., 1975. "Mini-mental state". A practical method for grading the cognitive state of patients for the clinician. J. Psychiatr. Res. 12, 189–198.

Gottstein, U., Muller, W., Berghoff, W., Gartner, H., Held, K., 1971. [Utilization of non-esterified fatty acids and ketone bodies in human brain]. Klin. Wochenschr. 49, 406–411.

Graham, M.M., Muzi, M., Spence, A.M., O'Sullivan, F., Lewellen, T.K., Link, J.M., Krohn, K.A., 2002. The FDG lumped constant in normal human brain. J. Nucl. Med. 43, 1157–1166.

Hasselbalch, S.G., Knudsen, G.M., Jakobsen, J., Hageman, L.P., Holm, S., Paulson, O.B., 1995. Blood-brain barrier permeability of glucose and ketone bodies during short-term starvation in humans. Am. J. Physiol. 268 (6 Pt 1), E1161–E1166.

Hasselbalch, S.G., Madsen, P.L., Hageman, L.P., Olsen, K.S., Justesen, N., Holm, S., Paulson, O.B., 1996. Changes in cerebral blood flow and carbohydrate metabolism during acute hyperketonemia. Am. J. Physiol. 270 (5 Pt 1), E746–E751.

Henderson, S.T., 2008. Ketone bodies as a therapeutic for Alzheimer's disease. Neurotherapeutics 5, 470–480. http://dx.doi.org/10.1016/j.nurt.2008.05.004.

Ibanez, V., Pietrini, P., Alexander, G.E., Furey, M.L., Teichberg, D., Rajapakse, J.C., Rapoport, S.I., Schapiro, M.B., Horwitz, B., 1998. Regional glucose metabolic abnormalities are not the result of atrophy in Alzheimer's disease. Neurology 50, 1585–1593.

Ibanez, V., Pietrini, P., Furey, M.L., Alexander, G.E., Millet, P., Bokde, A.L., Teichberg, D., Schapiro, M.B., Horwitz, B., Rapoport, S.I., 2004. Resting state brain glucose metabolism is not reduced in normotensive healthy men during aging, after correction for brain atrophy. Brain Res. Bull 63, 147–154. http://dx.doi.org/10.1016/j.brainresbull.2004.02.003.

Kalpouzos, G., Chetelat, G., Baron, J.C., Landeau, B., Mevel, K., Godeau, C., Barre, L., Constans, J.M., Viader, F., Eustache, F., Desgranges, B., 2009. Voxel-based mapping of brain gray matter volume and glucose metabolism profiles in normal aging. Neurobiol. Aging 30, 112–124. http://dx.doi.org/10.1016/j.neurobiolaging.2007.05.019.

Kantarci, K., Senjem, M.L., Lowe, V.J., Wiste, H.J., Weigand, S.D., Kemp, B.J., Frank, A.R., Shiung, M.M., Boeve, B.F., Knopman, D.S., Petersen, R.C., Jack Jr., C.R., 2010. Effects of age on the glucose metabolic changes in mild cognitive impairment. AJNR Am. J. Neuroradiol. 31, 1247–1253. http://dx.doi.org/10.3174/ajnr.A2070.

Krikorian, R., Shidler, M.D., Dangelo, K., Couch, S.C., Benoit, S.C., Clegg, D.J., 2012. Dietary ketosis enhances memory in mild cognitive impairment. Neurobiol. Aging 33, 425.e19–425.e27. http://dx.doi.org/10.1016/j.neurobiolaging.2010.10.006.

Laffel, L., 1999. Ketone bodies: a review of physiology, pathophysiology and application of monitoring to diabetes. Diabetes Metab. Res. Rev. 15, 412–426.

Langbaum, J.B., Chen, K., Lee, W., Reschke, C., Bandy, D., Fleisher, A.S., Alexander, G.E., Foster, N.L., Weiner, M.W., Koeppe, R.A., Jagust, W.J., Reiman, E.M., 2009. Categorical and correlational analyses of baseline fluorodeoxyglucose positron emission tomography images from the Alzheimer's Disease Neuroimaging Initiative (ADNI). Neuroimage 45, 1107–1116. http://dx.doi.org/10.1016/j.neuroimage.2008.12.072.

Li, Y., Rinne, J.O., Mosconi, L., Pirraglia, E., Rusinek, H., DeSanti, S., Kemppainen, N., Nagren, K., Kim, B.C., Tsui, W., de Leon, M.J., 2008. Regional analysis of FDG and PIB-PET images in normal aging, mild cognitive impairment, and Alzheimer's disease. Eur. J. Nucl. Med. Mol. Imaging 35, 2169–2181. http://dx.doi.org/10.1007/s00259-008-0833-y.

Lying-Tunell, U., Lindblad, B.S., Malmlund, H.O., Persson, B., 1981. Cerebral blood flow and metabolic rate of oxygen, glucose, lactate, pyruvate, ketone bodies and amino acids. Acta Neurol. Scand. 63, 337–350.

Maalouf, M., Rho, J.M., Mattson, M.P., 2009. The neuroprotective properties of calorie restriction, the ketogenic diet, and ketone bodies. Brain Res. Rev. 59, 293–315. http://dx.doi.org/10.1016/j.brainresrev.2008.09.002.

Mamelak, M., 2012. Sporadic Alzheimer's disease: the starving brain. J. Alzheimers Dis. 31, 459–474. http://dx.doi.org/10.3233/JAD-2012-120370.

Marano, C.M., Workman, C.I., Kramer, E., Hermann, C.R., Ma, Y., Dhawan, V., Chaly, T., Eidelberg, D., Smith, G.S., 2012. Longitudinal studies of cerebral glucose metabolism in late-life depression and normal aging. Int. J. Geriatr. Psychiatry. http://dx.doi.org/10.1002/gps.3840.

Mitchell, G.A., Kassovska-Bratinova, S., Boukaftane, Y., Robert, M.F., Wang, S.P., Ashmarina, L., Lambert, M., Lapierre, P., Potier, E., 1995. Medical aspects of ketone body metabolism. Clin. Invest. Med. 18, 193–216.

Morris, A.A., 2005. Cerebral ketone body metabolism. J. Inherit. Metab. Dis. 28, 109–121. http://dx.doi.org/10.1007/s10545-005-5518-0.

Mosconi, L., Brys, M., Switalski, R., Mistur, R., Glodzik, L., Pirraglia, E., Tsui, W., De Santi, S., de Leon, M.J., 2007. Maternal family history of Alzheimer's disease predisposes to reduced brain glucose metabolism. Proc. Natl. Acad. Sci. U.S.A 104, 19067–19072. http://dx.doi.org/10.1073/pnas.0705036104.

Mosconi, L., Mistur, R., Switalski, R., Tsui, W.H., Glodzik, L., Li, Y., Pirraglia, E., De Santi, S., Reisberg, B., Wisniewski, T., de Leon, M.J., 2009. FDG-PET changes in brain glucose metabolism from normal cognition to pathologically verified Alzheimer's disease. Eur. J. Nucl. Med. Mol. Imaging 36, 811–822. http://dx.doi.org/10.1007/s00259-008-1039-z.

Nehlig, A., 2004. Brain uptake and metabolism of ketone bodies in animal models. Prostaglandins Leukot. Essent. Fatty Acids 70, 265–275. http://dx.doi.org/10.1016/j.plefa.2003.07.006.

Owen, O.E., Morgan, A.P., Kemp, H.G., Sullivan, J.M., Herrera, M.G., Cahill Jr., G.F., 1967. Brain metabolism during fasting. J. Clin. Invest. 46, 1589–1595. http://dx.doi.org/10.1172/JCI105650.

Page, M.A., Williamson, D.H., 1971. Enzymes of ketone-body utilisation in human brain. Lancet 2, 66—68.

Patlak, C.S., Blasberg, R.G., Fenstermacher, J.D., 1983. Graphical evaluation of blood-to-brain transfer constants from multiple-time uptake data. J. Cereb. Blood Flow Metab. 3, 1—7. http://dx.doi.org/10.1038/jcbfm.1983.1.

Phelps, M.E., Huang, S.C., Hoffman, E.J., Selin, C., Sokoloff, L., Kuhl, D.E., 1979. Tomographic measurement of local cerebral glucose metabolic rate in humans with (F-18)2-fluoro-2-deoxy-D-glucose: validation of method. Ann. Neurol. 6, 371—388. http://dx.doi.org/10.1002/ana.410060502.

Pierre, K., Pellerin, L., 2005. Monocarboxylate transporters in the central nervous system: distribution, regulation and function. J. Neurochem. 94, 1—14. http://dx.doi.org/10.1111/j.1471-4159.2005.03168.x.

Pifferi, F., Tremblay, S., Croteau, E., Fortier, M., Tremblay-Mercier, J., Lecomte, R., Cunnane, S.C., 2011. Mild experimental ketosis increases brain uptake of 11C-acetoacetate and 18F-fluorodeoxyglucose: a dual-tracer PET imaging study in rats. Nutr. Neurosci. 14, 51—58. http://dx.doi.org/10.1179/1476830510Y.0000000001.

Quarantelli, M., Berkouk, K., Prinster, A., Landeau, B., Svarer, C., Balkay, L., Alfano, B., Brunetti, A., Baron, J.C., Salvatore, M., 2004. Integrated software for the analysis of brain PET/SPECT studies with partial-volume-effect correction. J. Nucl. Med. 45, 192—201.

Reger, M.A., Henderson, S.T., Hale, C., Cholerton, B., Baker, L.D., Watson, G.S., Hyde, K., Chapman, D., Craft, S., 2004. Effects of beta-hydroxybutyrate on cognition in memory-impaired adults. Neurobiol. Aging 25, 311—314. http://dx.doi.org/10.1016/S0197-4580(03)00087-3.

Reiman, E.M., Chen, K., Alexander, G.E., Caselli, R.J., Bandy, D., Osborne, D., Saunders, A.M., Hardy, J., 2004. Functional brain abnormalities in young adults at genetic risk for late-onset Alzheimer's dementia. Proc. Natl. Acad. Sci. U.S.A 101, 284—289. http://dx.doi.org/10.1073/pnas.2635903100.

Reiman, E.M., Chen, K., Alexander, G.E., Caselli, R.J., Bandy, D., Osborne, D., Saunders, A.M., Hardy, J., 2005. Correlations between apolipoprotein E epsilon4 gene dose and brain-imaging measurements of regional hypometabolism. Proc. Natl. Acad. Sci. U.S.A 102, 8299—8302. http://dx.doi.org/10.1073/pnas.0500579102.

Robinson, A.M., Williamson, D.H., 1980. Physiological roles of ketone bodies as substrates and signals in mammalian tissues. Physiol. Rev. 60, 143—187.

Roy, M., Nugent, S., Tremblay-Mercier, J., Tremblay, S., Courchesne-Loyer, A., Beaudoin, J.F., Tremblay, L., Descoteaux, M., Lecomte, R., Cunnane, S.C., 2012. The ketogenic diet increases brain glucose and ketone uptake in aged rats: a dual tracer PET and volumetric MRI study. Brain Res. 1488, 14—23. http://dx.doi.org/10.1016/j.brainres.2012.10.008.

Scheef, L., Spottke, A., Daerr, M., Joe, A., Striepens, N., Kolsch, H., Popp, J., Daamen, M., Gorris, D., Heneka, M.T., Boecker, H., Biersack, H.J., Maier, W., Schild, H.H., Wagner, M., Jessen, F., 2012. Glucose metabolism, gray matter structure, and memory decline in subjective memory impairment. Neurology 79, 1332—1339. http://dx.doi.org/10.1212/WNL.0b013e31826c1a8d.

Swerdlow, R.H., 2009. Mitochondrial Medicine and the Neurodegenerative Mitochondriopathies. Pharmaceuticals (Basel) 2, 150—167. http://dx.doi.org/10.3390/ph2030150.

Tremblay, S., Ouellet, R., Rodrigue, S., Langlois, R., Benard, F., Cunnane, S.C., 2007. Automated synthesis of 11C-acetoacetic acid, a key alternate brain fuel to glucose. Appl. Radiat. Isot. 65, 934—940. http://dx.doi.org/10.1016/j.apradiso.2007.03.015.

Vaishnavi, S.N., Vlassenko, A.G., Rundle, M.M., Snyder, A.Z., Mintun, M.A., Raichle, M.E., 2010. Regional aerobic glycolysis in the human brain. Proc. Natl. Acad. Sci. U.S.A 107, 17757—17762. http://dx.doi.org/10.1073/pnas.1010459107.

Veech, R.L., Chance, B., Kashiwaya, Y., Lardy, H.A., Cahill Jr., G.F., 2001. Ketone bodies, potential therapeutic uses. IUBMB Life 51, 241—247. http://dx.doi.org/10.1080/152165401753311780.

Veneman, T., Mitrakou, A., Mokan, M., Cryer, P., Gerich, J., 1994. Effect of hyperketonemia and hyperlacticacidemia on symptoms, cognitive dysfunction, and counterregulatory hormone responses during hypoglycemia in normal humans. Diabetes 43, 1311—1317.

Vlassenko, A.G., Vaishnavi, S.N., Couture, L., Sacco, D., Shannon, B.J., Mach, R.H., Morris, J.C., Raichle, M.E., Mintun, M.A., 2010. Spatial correlation between brain aerobic glycolysis and amyloid-β (Aβ) deposition. Proc. Natl. Acad. Sci. U.S.A 107, 17763—17767. http://dx.doi.org/10.1073/pnas.1010461107.

Willis, M.W., Ketter, T.A., Kimbrell, T.A., George, M.S., Herscovitch, P., Danielson, A.L., Benson, B.E., Post, R.M., 2002. Age, sex and laterality effects on cerebral glucose metabolism in healthy adults. Psychiatry Res. 114, 23—37.

Yanase, D., Matsunari, I., Yajima, K., Chen, W., Fujikawa, A., Nishimura, S., Matsuda, H., Yamada, M., 2005. Brain FDG PET study of normal aging in Japanese: effect of atrophy correction. Eur. J. Nucl. Med. Mol. Imaging 32, 794—805. http://dx.doi.org/10.1007/s00259-005-1767-2.

Yuan, X., Shan, B., Ma, Y., Tian, J., Jiang, K., Cao, Q., Wang, R., 2010. Multi-center study on Alzheimer's disease using FDG PET: group and individual analyses. J. Alzheimers Dis. 19, 927—935. http://dx.doi.org/10.3233/JAD-2010-1287.

Zhou, S., Chen, K., Reiman, E.M., Li, D.M., Shan, B., 2011. A method of generating image-derived input function in a quantitative (1)(8)F-FDG PET study based on the shape of the input function curve. Nucl. Med. Commun. 32, 1121—1127. http://dx.doi.org/10.1097/MNM.0b013e32834abd1b.